Catalysis Science & Technology

ROYAL SOCIETY OF CHEMISTRY

PAPER

View Article Online
View Journal

Cite this: DOI: 10.1039/d0cy01008a

Mechanistic insight into the azo radical-promoted dehydrogenation of heteroarene towards N-heterocycles†

Amreen K. Bains and Debashis Adhikari *

Received 17th May 2020,
Accepted 20th July 2020

DOI: 10.1039/d0cy01008a

rsc.li/catalysis

Borrowing hydrogenation-promoted annulations are considered to be important reactions to synthesize wide variety of N-heterocycles. In these processes, the dehydrogenation of saturated heteroarenes in the late stage is generally required to furnish the desired N-heterocycle. However, in a one-pot, multistep heterocycle synthesis, this step is not well elucidated, and the role of the catalyst is not thoroughly understood. Furthermore, the use of copious amount of base at elevated temperatures further complicates this matter and casts doubt on the involvement of the catalyst in heteroarene dehydrogenation. Herein, we report a molecularly defined nickel catalyst, which can perform two annulation reactions under mild conditions (80 °C, 8 h), towards the sustainable synthesis of triazine and pyrimidine. Mechanistically, we clearly describe the important role of the catalyst in promoting the dehydrogenation of heteroarenes. The binding of the saturated heterocycle to the metal catalyst undergoes a pre-equilibrium step (K = 238 at 80 °C), which is followed by a crucial hydrogen atom transfer. A series of kinetics experiments including Van't Hoff, Eyring analysis and interception of pyrimidinyl radical disclosed the details of the dehydrogenation process. This ligand-driven, base metal catalytic approach is significantly different from the considerably evaluated metal–ligand cooperative bond activation strategies, which may offer an alternative dehydrogenation pathway that demands less energy.

Introduction

The new discovery of reactions that can transform alcohols to important value-added products greatly contributes towards sustainability by preserving fossil fuel reserves. The convenient and cheap sources of alcohol are indigestible biomass, which makes this substrate an attractive chemical feedstock.[1] Accordingly, hydrogen borrowing (HB) from alcohols,[2–8] also known as hydrogen auto-transfer, has emerged as a fascinating methodology to fabricate a multitude of important organic molecules including N-heterocycles.[9–13] Aromatic N-heterocycles are ubiquitously present in natural products, pharmaceutically important molecules and organic functional materials.[14] The previously reported methods to assemble these heteroarenes include dehydrogenation of the corresponding saturated N-heterocycles using a stoichiometric oxidant.[15] In contrast, catalytic acceptorless dehydrogenations are much more atom efficient and have the added advantage of extruding H_2 during desaturation. However, it is important to understand the different pathways for this dehydrogenation since saturated heterocycles are regarded as organic liquid hydrogen carriers, and thus attracts significant attention from researchers.[16]

In the case of a one-pot, multi-component reaction towards the synthesis of value-added N-heterocycle products, dehydrogenation of the substrates is critical. The success of multiple catalysts in homogeneous de/hydrogenation catalysis is strongly governed by designer ligands, where the metal–ligand scaffold activates a bond *via* a cooperative action.[17,18] Noyori,[19] Shvo,[20] and Milstein[21] showcased elegant examples where the dehydrogenation reaction of an alcohol is promoted by the tandem activation of two bonds by a metal and a heteroatom or aromatization–dearomatization (Scheme 1). Using metal–ligand cooperativity, Fujita and Yamaguchi developed an efficient Ir-catalyst that dehydrogenated 1,2,3,4-tetrahydroquinolines and other cyclic amines.[22] Subsequently, Crabtree and Jones studied several dehydrogenation reactions of N-heterocycles, which have a similar underlying activation principle, but the active catalysts are based on nickel,[23] iron,[24] and cobalt.[2] Analogous to these metal-catalyzed efforts, the recent approach of frustrated Lewis pair-based dehydrogenation of heteroarenes has also attracted significant attention.[25–27]

Department of Chemical Sciences, Indian Institute of Science Education and Research (IISER) Mohali, SAS Nagar-140306, India. E-mail: adhikari@iisermohali.ac.in

† Electronic supplementary information (ESI) available: Experimental procedure, spectroscopic and kinetic data. See DOI: 10.1039/d0cy01008a

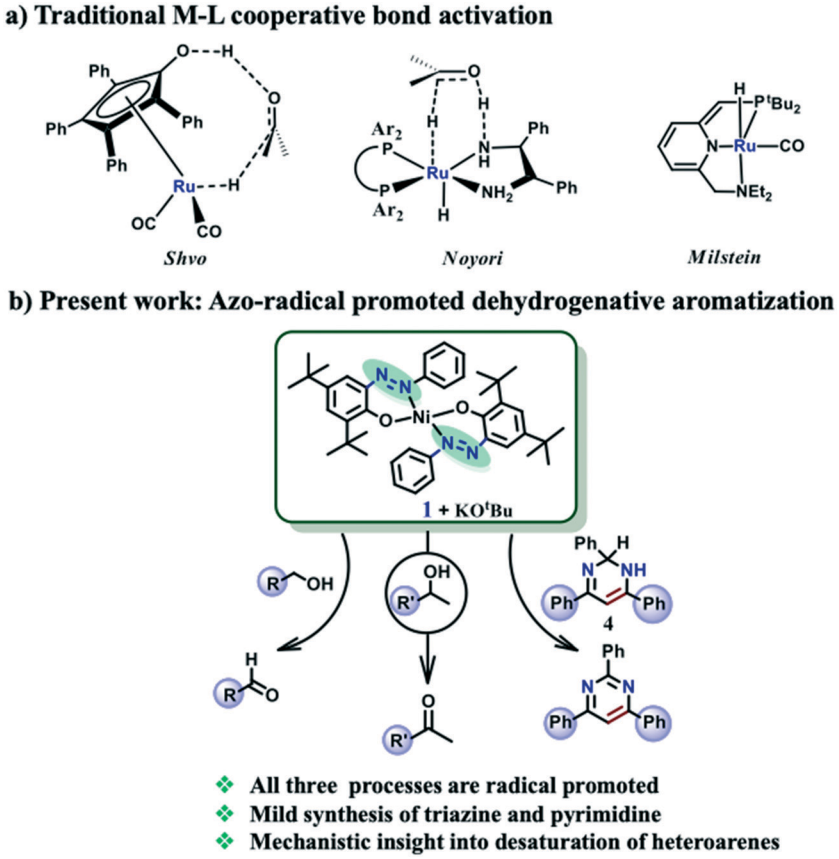

Scheme 1 Traditional M–L bifunctionality bond activation *vs.* azo radical-promoted dehydrogenation reactions.

However, despite the attempts to understand the dehydrogenation of heteroarenes, there is still a lack of precise knowledge, especially where an N-heterocycle is isolated from a one-pot reaction. The seminal works reported by the abovementioned groups examined dehydrogenations on a pre-synthesized molecule. In contrast, when a one-pot, multi-step reaction furnishes value-added heterocycles *via* a series of oxidation, condensation, and dehydrogenation reactions, clear mechanistic details of the late stage dehydrogenation of heteroarenes are often lacking. In several examples, the reaction is performed at high temperature for an extended reaction time in the presence of a base. Thus, whether the catalyst plays a critical role in bond activations towards dehydrogenation or it is simply driven by gaining aromaticity, is a matter of considerable speculation. Furthermore, a simple base-promoted dehydrogenation under a high loading of base and elevated temperature, as recently reported by Yu, complicates this issue further.[28] Herein, we attempt to understand the dehydrogenation of heteroarenes, where HB methods from alcohols are employed. We recently discovered a nickel complex with a redox-active azophenolate backbone that promotes facile alcohol oxidation enroute to the *N*-alkylation of amines and the formation of benzazoles.[29,30] We aim to showcase that the same catalyst can also furnish two N-heterocycles under very mild reaction conditions and provide the opportunity to study the dehydrogenation pathway of saturated heteroarenes. As will be delineated through further studies, the reaction is completely radical mediated, and contrasts heavily with the earlier examples of the dehydrogenation of heterocycles *via* metal–ligand cooperative action.

Results and discussion

Recently, we established that the proximity of the two azo functionalities to nickel in **1** is instrumental for alcohol oxidation to occur *via* the radical pathway employing a hydrogen atom transfer (HAT) event.[29] During this process, we further proved that the azo radical was generated by a very mild reductant such as KO^{t}Bu, which was feasible due to the low-lying π^* of the nickel-bound azo moiety.

Encouraged by the dehydrogenating ability of **1**, we proposed a two-component coupling of alcohol with amidinate salt, and subsequent dehydrogenation resulting in triazines.[31,32] It is well known that aryl-substituted 1,3,5-triazine derivatives exhibit diverse biological activities.[33] Thus, to test the viability of the assumed synthetic protocol, a model reaction was performed in the presence of benzyl alcohol and amidinate salt. Gratifyingly, different triazine cores were readily synthesized *via* the condensation of aldehydes with amidinates at a mild reaction temperature of 80 °C. A series of control experiments were performed, which clearly support the

necessity of both catalyst and base for the success of this reaction. Several functional groups with both electron donating such as –OMe (**2b**) and –Me (**2c**) and withdrawing substituents –Cl (**2d**), –Br (**2e**), and –F (**2f**) at the *para*-positions of the benzyl alcohol gave the respective triazine products in good yield (66–82%) (**2a–2f**, Table 1) within a reaction time of 8 h. Notably, the reaction was performed under aerobic conditions by keeping an oxygen-filled balloon on the reaction flask.

Next, we anticipated that a similar three-component coupling by **1** including primary and secondary alcohols and an amidine will result in pyrimidine. Pyrimidine is a very important heterocycle, which is present in DNA base pairs and exhibits notable biological activity. This type of three-component coupling was first reported by Kempe and co-workers using an iridium catalyst at high reaction temperature.[34] Further developments included many base metals and modified conditions, but the details of dehydrogenating saturated heteroarenes enroute to pyrimidine was not explored thoroughly.[35–38] We commenced our synthesis of pyrimidine using benzyl alcohol, 1-phenyl ethanol and benzamidinate salt as prototypical substrates. Gratifyingly, the reaction mixture when heated at 80 °C for 8 h, conveniently resulted in the corresponding pyrimidine in 90% yield. The optimized conditions revealed that 5% catalyst loading was required to obtain best yield, while the optimum base loading was 0.5 equivalent (Table S1, ESI†). An array of control experiments justified the requirement of both catalyst and base for the success of the reaction. Notably, in our optimized reaction conditions, the temperature and reaction time are significantly reduced compared to other catalysts towards the synthesis of pyrimidine, which we attribute to the low-energy reaction pathway.[34–36] To scrutinize the homogeneous nature of this catalyst, a mercury test was performed, which did not have any adverse effect on the reaction outcome (ESI,† section 2E). Furthermore, the clear first order dependence of the reaction rate on catalyst concentration also attests to the homogeneous nature of the reaction. The generality of the synthetic method was further tested with an array of primary alcohols. Primary alcohols with different halides, such as –F and –Cl were well tolerated, giving excellent yields of the corresponding pyrimidines (Table 2, **3g–i**). Furthermore, naphthyl-1-methanol afforded the respective pyrimidine (**3d**) in 88% yield. Simple alkyl substituents including –Me and –^{i}Pr at the *p*-position of the benzyl alcohol, all assembled the respective pyrimidine (**3b** and **3f**) in good to excellent yield. Notably, this reaction was also performed under neat oxygen conditions with an oxygen balloon added to the neck of the reaction flask. The presence of pure oxygen during the reaction had a strong influence on the regeneration of the catalyst. We will further discuss the effect of the catalyst and the reaction pathway to turn the overall conditions to be a milder one.

To further expand the substrate scope of the reaction, a diverse range of amidines was examined. Encouragingly, methyl

Table 1 Synthesis of 1,3,5-triazine

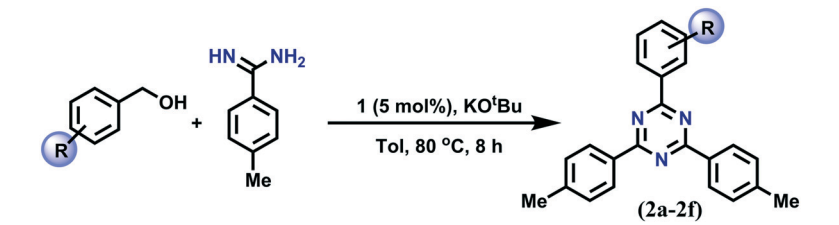

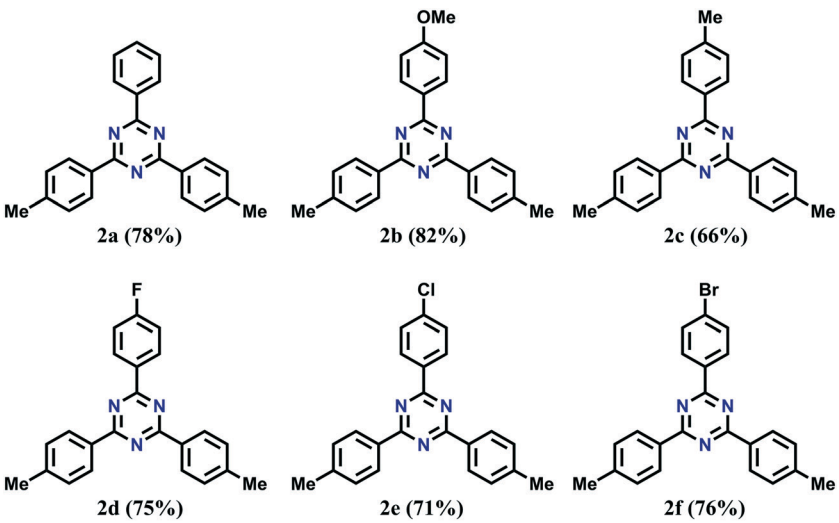

Reaction conditions: **1** (5 mol%), primary alcohols (0.5 mmol), 4-methyl benzamidine (1 mmol), KO^{t}Bu (0.5 mmol), toluene (2 mL), 80 °C, 8 h, and O_2 balloon (isolated yield).

Table 2 Synthesis of pyrimidine with diverse alcohols and amidines

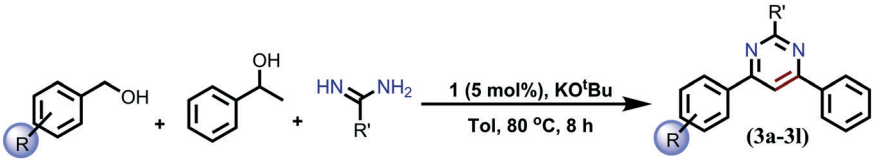

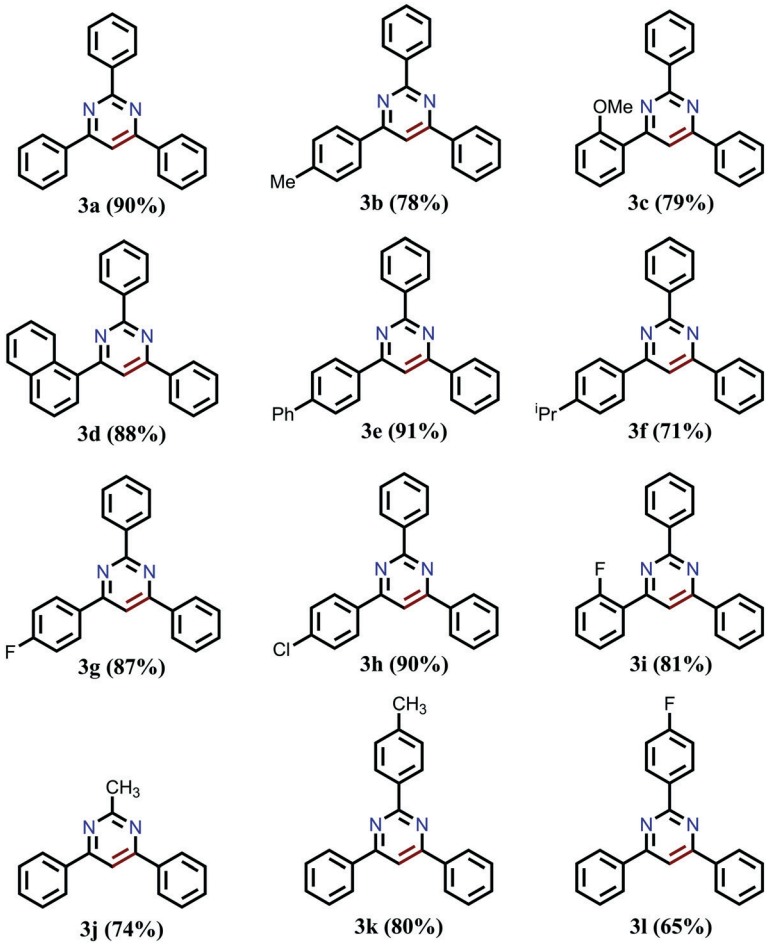

Reaction conditions: **1** (5 mol%), primary alcohols (1 mmol), 1-phenyl ethanol (1.25 mmol), amidines (1 mmol), KO^{t}Bu (0.5 mmol), toluene (2 mL), 80 °C, 8 h, O_2 balloon (isolated yield).

amidinate smoothly furnished the 2-Me-4,6-phenyl pyrimidine (**3j**, Table 2) in 74% yield under the optimized reaction conditions. Additionally, *p*-substituted aryl amidines with a highly electron withdrawing fluoro group offered the corresponding pyrimidine (**3l**) in 65% yield. Similarly, *p*-tolyl amidine offered the respective pyrimidine ring (**3k**) in very good yield.

Mechanistic study towards dehydrogenation of dihydropyrimidine (4)

As described previously, the presence of the redox-active azo functionality in the ligand backbone facilitates the oxidation of a substrate *via* HAT.[29] Towards the synthesis of pyrimidine, a total of 2 molecules of H_2O and 3 molecules of H_2 are eliminated (in the form of H_2O_2) during the three-component coupling. Hydrogen molecules are trapped in the catalyst backbone during alcohol oxidation, and in the final step, the dehydrogenative aromatization of the N-heterocycle occurs. Our previous study clearly disclosed that alcohols can be readily oxidized under fairly mild reaction conditions. Cross-aldol condensation between benzaldehyde and acetophenone followed by nucleophilic attack of the amidine results in 1,2-dihydropyrimidine, **4** (Scheme 3a, *vide infra*). We were very intrigued by the dehydrogenation process of **4** in this study. Thus, to prove that the dehydrogenation is an important step in the formation of pyrimidine, we synthesized the methylated analogue of **4** starting from 1-phenyl ethanol, and isolated the intermediate in the final stage (Scheme 2b and Fig. S2, ESI†). Conceivably, the oxidative dehydrogenation of **4** requires more energy than the other steps involved in the synthesis of

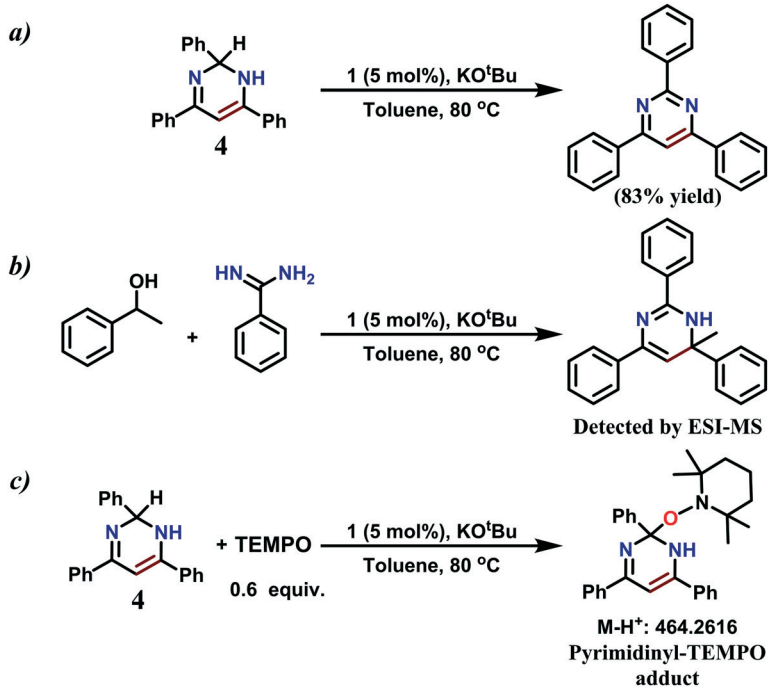

Scheme 2 a) Dehydrogenative aromatization of **4** under the optimized reaction conditions. b) Arrested methylated analogue of **4**. c) Pyrimidinyl-TEMPO adduct formation.

pyrimidine. In fact, with the present catalyst system, both primary and secondary alcohols can be oxidized at 50 °C within 2 h. In many previously reported pyrimidine syntheses, the reaction temperature was usually maintained at 120–140 °C.[34,36] However, the mechanism of the heterocycle dehydrogenation reaction at elevated temperatures has thus far not been thoroughly investigated. Whether the purported Mn, Ir, or Cu catalyst has a specific role towards this dehydrogenation of dihydropyrimidine or base promotes the dehydrogenation at elevated temperature is not very clear.[38] This is also indirectly supported by the observation of Srimani, where 2,3-dihydroperimidine was isolated under Mn-catalyzed conditions at 120 °C, whereas no dehydrogenated pyrimidine was isolated.[39] This observation is consistent with the difficulty associated with producing pyrimidines from dihydropyrimidines owing to the unfavorable change in enthalpy. As we discussed earlier, our optimized temperature and reaction time were reduced considerably, and we surmise that catalyst **1** has a specific role in this dehydrogenation reaction. Previously, a ruthenium and heterogeneous platinum-catalyzed pyrimidine synthesis also alluded to the role of the catalyst in 2,3-dihydropyrimidine dehydrogenation, but did not present the detailed steps.[40,41]

The understanding of the detailed mechanism for dehydrogenative aromatization has been often overlooked to date. Sometimes pure aerial oxidation of the dihydropyrimidine has been assumed as a possible route to its unsaturated analogue, which is clearly not a facile process.[38] In good agreement with our proposed hypothesis, the conversion of **4** to the aromatic pyrimidine is a background reaction when the reaction was conducted at 80 °C without any catalyst (Fig. 1). This observation corroborates well with the base-promoted dehydrogenation of saturated heteroarenes reported recently. Indolines and 1,2,3,4-tetrahydroqunolines were dehydrogenated to indoles and quinolines, respectively, under severe conditions of 2–3 equivalent of KO^{t}Bu and heating at 140 °C for 36 h when no catalyst was present.[28]

To investigate the dehydrogenation of **4** in detail using our catalyst system, we pre-synthesized the molecule and studied the detailed kinetics of the dehydrogenation reaction. Initially, to ensure that **4** requires binding to nickel during the dehydrogenation step, we monitored the increase in the observed rate constant (k_{obs}) with a gradual increase in the concentration of **4**. The two rate constants used in this discussion are k_{obs}, which is the measured rate under pseudo-first-order condition of substrate, and the derived first-order rate constant k for the HAT step. This experiment clearly displayed the saturation behavior of **4** at higher concentration and unambiguously authenticated that the binding is important (Fig. 2a). The saturation behavior was modeled *via* the pre-equilibrium step following eqn (1), and non-linear curve fitting provided the equilibrium constant of 238 M^{-1} at 80 °C.

$$[1]^{\bullet -} + 4 \overset{K}{\rightleftharpoons} [1{\cdot}4]^{\bullet -} \xrightarrow{k} \text{Product} \qquad (1)$$

$$k_{obs} = \frac{kK[4]}{1 + K[4]}$$

The fitting also gave the first-order rate constant, $k = 9.1 \times 10^{-4}$ s^{-1} for the subsequent process, which is HAT to the azo radical. We studied the pre-equilibrium behavior of **4** under dehydrogenation at three different temperatures, which

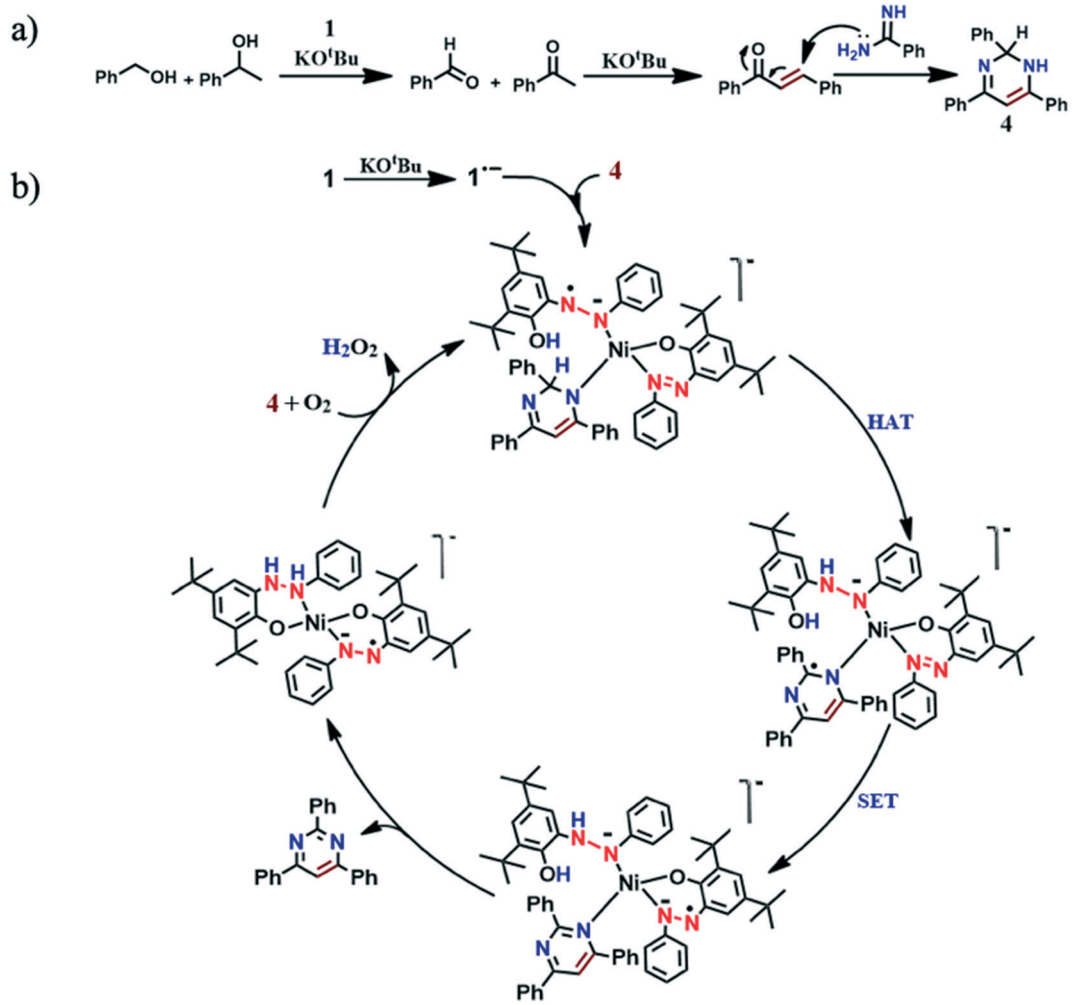

Scheme 3 a) Schematic representation for the formation of **4** *via* the oxidation of alcohols and subsequent Claisen–Schmidt condensation. b) Plausible mechanism for the azo radical mediated dehydrogenation of **4** *via* a critical hydrogen atom transfer step.

followed the expected trend of a decrease in the equilibrium constant at higher temperature (Table 3). The calculated equilibrium constants at different temperatures and their plots of natural logarithm with respect to inverse temperature disclosed $\Delta H°$ and $\Delta S°$ to be −5.74 kcal mol^{-1} and −3.34 cal mol^{-1} K^{-1} respectively (Fig. 2b) based on the Van't Hoff equation. The moderate value of the enthalpy change can be ascribed to the simultaneous protonation of the phenolate arm

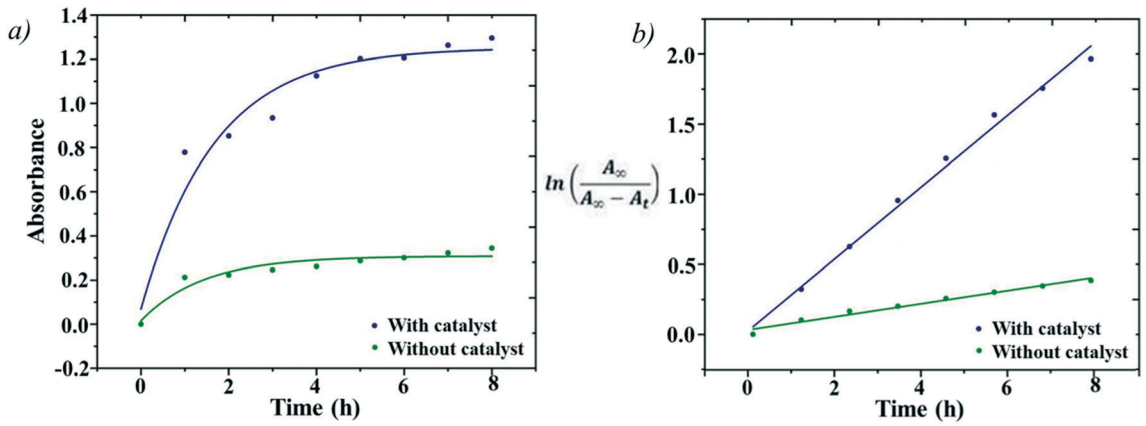

Fig. 1 Kinetic analysis for the dehydrogenation of **4** in the presence and absence of catalyst. a) Product growth with time, reaction temperature 80 °C. b) Calculation of pseudo-first-order rate constant.

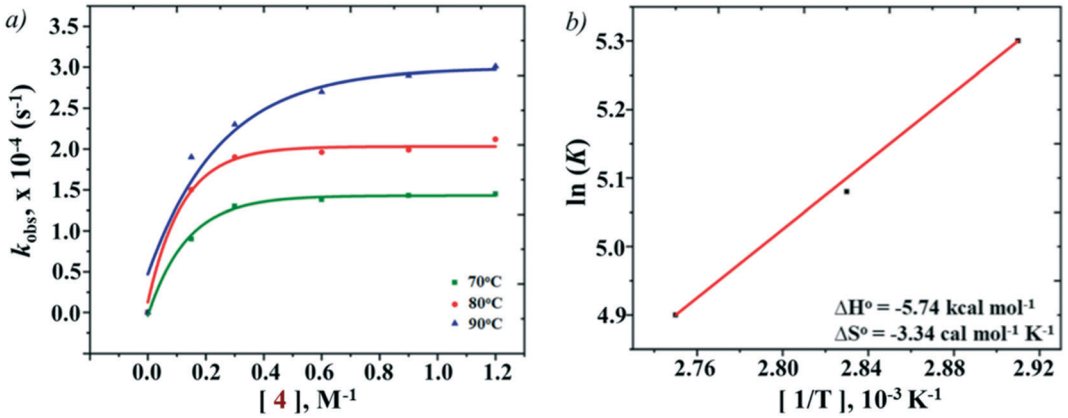

Fig. 2 a) Saturation kinetics profile for the binding of **4** to **1**, at three different temperatures, b) Van't Hoff plot from equilibrium constant data.

and its detachment to nickel during the binding of **4** to the complex (Scheme 3b). The overall $\Delta S°$ for the formation of the complex is also the sum of several entropy changes with different signs. The loss of entropy accompanies the restriction due to binding of **4**, while an increase in entropy occurs when the phenol arm detaches from the metal center.

Interestingly, the pseudo-first-order rate of dehydrogenation for **4** at 80 °C under oxygenated conditions is 9.1×10^{-4} s^{-1}, while that at the same temperature without any catalyst is only 1.6×10^{-6} s^{-1}. Thus, the rate enhancement for the dehydrogenation of **4** in the presence of the catalyst is at least 550 times. However, in the absence of catalyst **1** (but in the presence of 0.5 equiv. of base) the rate of dehydrogenation reached the observed rate only when the temperature was elevated to 140–150 °C (Fig. S5, ESI†). Moreover, to authenticate the feasibility of the dehydrogenation at the reaction temperature (80 °C), we performed an Eyring analysis with the first-order rate constants. The Eyring plot conveyed $\Delta H^{\ddagger}$ of 20.23 ± 1.83 kcal mol^{-1}, while $\Delta S^{\ddagger}$ to be −24.98 ± 0.94 cal mol^{-1} K^{-1} (Fig. 3). The negative $\Delta S^{\ddagger}$ value indicates the bimolecular nature of the dehydrogenation step, where **4** binds to reduced **1**. The overall reaction barrier, $\Delta G^{\ddagger}$ of 29.05 ± 2.81 kcal mol^{-1}, for the process calculated at 80 °C is consistent with the dehydrogenation of **4** proceeding under our reaction conditions.

Considering the reduced azo functionality as a ligand arm, we proved earlier that HAT is a facile process.[29] In the case of the oxidative dehydrogenation processes, the utility of the redox process is dependent on the C–H bond being broken. It can be anticipated that the C–H bond in the present case is benzylic in nature, and hence weak. Likewise, HAT from **4** will generate a transient carbene radical, which upon reducing the second unreduced azo arm, will generate pyrimidine. The proton transfer from phenol to nitrogen completes the reduction of the azo and leaves it with a hydrazo form (Scheme 3b). The hydrazo form of the catalyst was isolated and authenticated by NMR spectroscopy. Overall, the two-electron azo/hydrazo redox couple that can interconvert in a reversible fashion facilitates the dehydrogenation step required in this reaction.[42]

Further, to unambiguously ascertain that the dehydrogenation is radical mediated, we tried to quench the reaction in the presence of a well-known radical quencher, TEMPO (TEMPO = 2,2,6,6-tetramethylpiperidinyloxy), and observed significant quenching of the reaction (section 2B and C, ESI†). Moreover, the pyrimidinyl radical generated upon HAT can be intercepted as a TEMPO-adduct. The adduct was easily traced at 464.2616 amu in high-resolution mass-spectrometry, further providing compelling evidence for

Table 3 First-order rate constants and equilibrium constants at different temperatures for the aromatic dehydrogenation of **4** by **1**

S. No	Temperature (°C)	k (s^{-1})	K (M^{-1})
1.	70	1.1×10^{-4}	253
2.	80	9.1×10^{-4}	238
3.	90	5.4×10^{-3}	217

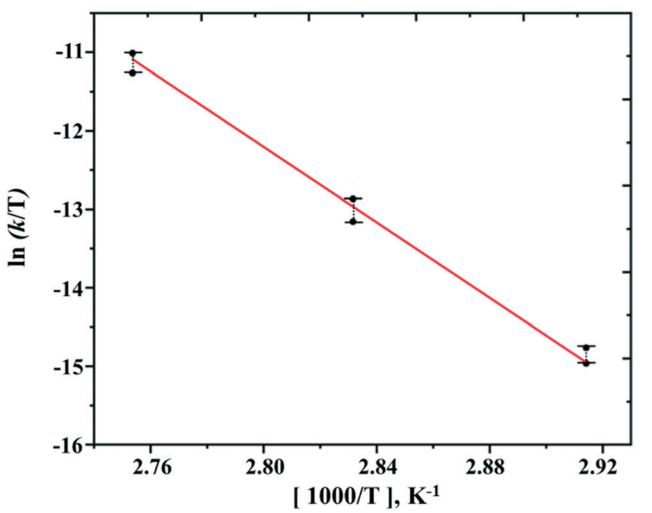

Fig. 3 Plot of ln(k/T) against 1/T to determine the activation parameters for the dehydrogenation of **4**.

the generation of the pyrimidinyl radical upon HAT (Fig. S3, ESI†). This type of radical-mediated aromatic dehydrogenation is extremely rare and only has few precedence in photocatalyzed reactions.[43,44] Furthermore, the dehydrogenation reactions totally circumventing the formation of metal hydride may possibly make this protocol tolerant to diversely functionalized N-heterocycles. It is known that the stability of 3d transition metal-based hydrides is poor, which affects the reaction conditions in an adverse way, and thus becomes problematic for sensitive functionalities.[45] Another advantage of our catalyst is the easy conversion of the hydrazo form to the catalytic resting state, the azo form, by simple oxidation with O_2. During the catalyst regeneration, H_2O_2 is formed as a by-product, which was detected *via* iodometry. The moderate energy demand for the crucial HAT step during the dehydrogenation and the ease of catalyst regeneration *via* oxidation by O_2 make the reaction conditions milder compared to that in many prior reports on the transition metal-catalyzed formation of heterocycles. It is also noteworthy that the dehydrogenation of the dihydropyrimidine adopting a radical pathway is completely different from the typical metal–ligand cooperative bond activation and offers an alternative desaturation pathway.[46–53] Although we did not describe the mechanistic details for the formation of triazine, a similar late-stage dehydrogenative aromatization of N-heterocycle is required (Scheme S1, ESI†), and thus it is anticipated that the catalyst functions in a similar manner.

Conclusion

In summary, the nickel catalyst presented herein can be employed to easily synthesize triazine and pyrimidine *via* dehydrogenative annulation reactions. The reaction conditions for the synthesis of pyrimidine are fairly mild and can truly rival the precious metal catalysts employed for this process. The azo motif in the ligand backbone has a vital role in the HAT-based oxidation and trapping the borrowed hydrogen, which obviates the need for a sacrificial acceptor molecule. Specifically, the easy oxidation of both primary and secondary alcohols and regeneration of the catalyst by oxidizing the trapped hydrogen in the form of H_2O_2 are the key factors for reducing the reaction time and temperature considerably. Furthermore, the dehydrogenative aromatization step, which is often required during the last phase in the formation of heterocycles, is assisted by the generation of a radical due to HAT. This study sheds light on the dehydrogenation of saturated heteroarenes and proves that the catalyst plays an important role in this specific step compared to base-promoted dehydrogenation at high temperature. Our synthetic protocol can also be a complementary route to the well-investigated metal–ligand cooperative bond activation towards dehydrogenation reactions.[2,54] Moreover, there is a strong current interest to accomplish asymmetric transformations utilizing the HB methodology. However, the usual high temperature requirement for HB-based methods poses a significant challenge to control the stereoselection.[9] Thus, the considerably milder reaction conditions achieved using the present method can ideally help in further controlling the stereoselectivity.

Experimental

General information

All reactants employed in this study were procured from commercial suppliers. Potassium *tert*-butoxide and potassium hydroxide were purchased from Sigma Aldrich. Primary alcohols, secondary alcohols, and amidines were purchased from Tokyo Chemical Industry (TCI). Glassware was dried overnight at 160 °C in an oven prior to use for the reactions. Methanol was used as received. Toluene was dried by heating over sodium with benzophenone. For thin layer chromatography (TLC), aluminum foil coated with silica and fluorescent indicator (from Merck) were used. Column chromatography was performed using silica gel 60–120 mesh using ethyl acetate and hexane as the mobile phase. High-resolution mass spectra were recorded on a Waters QTOF mass spectrometer. ^{1}H NMR and ^{13}C NMR spectra were recorded on a 400 MHz Bruker Biospin Advance III FT-NMR spectrometer. Proton chemical shifts were internally referenced to the residual proton signal in $CDCl_3$ (δ 7.26 ppm). Carbon chemical shifts were internally referenced to the deuterated solvent signals in $CDCl_3$ (δ 77.1 ppm). 1,4-Dihyro-2,4,6-triphenyl-pyrimidine (**4**) was synthesized according to the reported procedure.[55]

Synthesis of 1

A methanolic solution of **L** (0.1 mmol) was placed in a 50 mL round-bottom flask, KOH (0.1 mmol) was added and the mixture was stirred for 30 min. $Ni(OAc)_2$ (0.05 mmol) was added to the reaction mixture and refluxed for another 30 min. The precipitate was filtered. A dark brown product was obtained in 82% yield.

General procedure for N-heterocycle formation

1. General procedure for the synthesis of 1,3,5-triazines

A 5 mL vial was charged with alcohols (0.5 mmol), 4-methylbenzamidine hydrochloride (1 mmol), KO^{t}Bu (0.5 mmol), and **1** (5 mol%) in 2 mL toluene. The resulting solution was kept under a balloon filled with O_2. The reaction mixture was stirred at 80 °C for 8 h. Upon completion, the reaction mixture was cooled to room temperature and concentrated *in vacuo*. The crude mixture was purified by column chromatography using ethyl acetate/petroleum ether (15–20%) as the eluent to afford pure products. The desired product was characterized by ^{1}H and ^{13}C NMR spectroscopies.

2. General procedure for the synthesis of pyrimidine

A 5 mL vial was charged with alcohols (1 mmol), 1-phenylethanol (1.25 mmol), amidine hydrochloride (1 mmol), KO^{t}Bu (0.5 mmol), and **1** (5 mol%) in 2 mL toluene. The resulting solution was kept under a balloon filled with O_2. The reaction mixture was stirred at 80 °C for 8 h. The reaction mixture was cooled to room temperature and concentrated *in vacuo*. The crude mixture was purified by column chromatography using ethyl acetate/petroleum ether (15–20%) as the eluent to afford pure products. The desired product was characterized by ^{1}H and ^{13}C NMR spectroscopies.

Conflicts of interest

The authors declare no competing financial interests.

Acknowledgements

We thank SERB (DST), India (Grant No. ECR/2017/001764) for financial support and IISER Mohali for start-up funding. The central facility in IISER Mohali is acknowledged for NMR and HRMS measurements. AKB thanks IISER Mohali for a research fellowship. The authors thank Sudha Yadav for help in kinetic experiments and analysis.

References

1 C. O. Tuck, E. Pérez, I. T. Horváth, R. A. Sheldon and M. Poliakoff, *Science*, 2012, **337**, 695–699.
2 R. Xu, S. Chakraborty, H. Yuan and W. D. Jones, *ACS Catal.*, 2015, **5**, 6350–6354.
3 M. K. Barman, A. Jana and B. Maji, *Adv. Synth. Catal.*, 2018, **360**, 3233–3238.
4 D. Srimani, Y. Ben-David and D. Milstein, *Chem. Commun.*, 2013, **49**, 6632–6634.
5 B. Emayavaramban, M. Sen and B. Sundararaju, *Org. Lett.*, 2017, **19**, 6–9.
6 M. Zhang, X. Fang, H. Neumann and M. Beller, *J. Am. Chem. Soc.*, 2013, **135**, 11384–11388.
7 M. Zhang, H. Neumann and M. Beller, *Angew. Chem., Int. Ed.*, 2013, **52**, 597–601.
8 B. G. Reed-Berendt, K. Polidano and L. C. Morrill, *Org. Biomol. Chem.*, 2019, **17**, 1595–1607.
9 A. Corma, J. Navas and M. J. Sabater, *Chem. Rev.*, 2018, **118**, 1410–1459.
10 R. H. Crabtree, *Chem. Rev.*, 2017, **117**, 9228–9246.
11 T. Irrgang and R. Kempe, *Chem. Rev.*, 2019, **119**, 2524–2549.
12 K. Tokmic, C. R. Markus, L. Zhu and A. R. Fout, *J. Am. Chem. Soc.*, 2016, **138**, 11907–11913.
13 L. V. A. Hale, T. Malakar, K.-N. T. Tseng, P. M. Zimmerman, A. Paul and N. K. Szymczak, *ACS Catal.*, 2016, **6**, 4799–4813.
14 X. L. Hou, Z. Yang and H. N. C. Wong, *Progress in Heterocyclic Chemistry*, Pergamon, Oxford, 2005.
15 S. A. Girard, H. Huang, F. Zhou, G.-J. Deng and C.-J. Li, *Org. Chem. Front.*, 2015, **2**, 279–287.
16 R. H. Crabtree, *ACS Sustainable Chem. Eng.*, 2017, **5**, 4491–4498.
17 T. Zell and D. Milstein, *Acc. Chem. Res.*, 2015, **48**, 1979–1994.
18 P. A. Dub and J. C. Gordon, *ACS Catal.*, 2017, **7**, 6635–6655.
19 R. Noyori, C. A. Sandoval, K. Muñiz and T. Ohkuma, *Philos. Trans. R. Soc., A*, 2005, **363**, 901–912.
20 Y. Shvo, D. Czarkie, Y. Rahamim and D. F. Chodosh, *J. Am. Chem. Soc.*, 1986, **108**, 7400–7402.
21 C. Gunanathan and D. Milstein, *Acc. Chem. Res.*, 2011, **44**, 588–602.
22 R. Yamaguchi, C. Ikeda, Y. Takahashi and K.-I. Fujita, *J. Am. Chem. Soc.*, 2009, **131**, 8410–8412.
23 O. R. Luca, D. L. Huang, M. K. Takase and R. H. Crabtree, *New J. Chem.*, 2013, **37**, 3402–3405.
24 S. Chakraborty, W. W. Brennessel and W. D. Jones, *J. Am. Chem. Soc.*, 2014, **136**, 8564–8567.
25 M. Kojima and M. Kanai, *Angew. Chem., Int. Ed.*, 2016, **55**, 12224–12227.
26 A. F. G. Maier, S. Tussing, T. Schneider, U. Flörke, Z.-W. Qu, S. Grimme and J. Paradies, *Angew. Chem., Int. Ed.*, 2016, **55**, 12219–12223.
27 M. M. Guru, S. De, S. Dutta, D. Koley and B. Maji, *Chem. Sci.*, 2019, **10**, 7964–7974.
28 T. Liu, K. Wu, L. Wang and Z. Yu, *Adv. Synth. Catal.*, 2019, **361**, 3958–3964.
29 A. K. Bains, A. Kundu, S. Yadav and D. Adhikari, *ACS Catal.*, 2019, **9**, 9051–9059.
30 A. K. Bains, D. Dey, S. Yadav, A. Kundu and D. Adhikari, *Catal. Sci. Technol.*, 2020, DOI: 10.1039/d0cy00748j.
31 F. Xie, M. Chen, X. Wang, H. Jiang and M. Zhang, *Org. Biomol. Chem.*, 2014, **12**, 2761–2768.
32 W. Guo, M. Zhao, W. Tan, L. Zheng, K. Tao and X. Fan, *Org. Chem. Front.*, 2019, **6**, 2120–2141.
33 B. Klenke, M. Stewart, M. P. Barrett, R. Brun and I. H. Gilbert, *J. Med. Chem.*, 2001, **44**, 3440–3452.
34 N. Deibl, K. Ament and R. Kempe, *J. Am. Chem. Soc.*, 2015, **137**, 12804–12807.
35 M. Mastalir, M. Glatz, E. Pittenauer, G. Allmaier and K. Kirchner, *J. Am. Chem. Soc.*, 2016, **138**, 15543–15546.
36 N. Deibl and R. Kempe, *Angew. Chem., Int. Ed.*, 2017, **56**, 1663–1666.
37 R. Mondal, S. Sinha, S. Das, G. Chakraborty and N. D. Paul, *Adv. Synth. Catal.*, 2020, **362**, 594–600.
38 T. Shi, F. Qin, Q. Li and W. Zhang, *Org. Biomol. Chem.*, 2018, **16**, 9487–9491.
39 K. Das, A. Mondal, D. Pal, H. K. Srivastava and D. Srimani, *Organometallics*, 2019, **38**, 1815–1825.
40 M. Maji and S. Kundu, *Dalton Trans.*, 2019, **48**, 17479–17487.
41 S. Sultana Poly, S. M. A. H. Siddiki, A. S. Touchy, K. W. Ting, T. Toyao, Z. Maeno, Y. Kanda and K.-I. Shimizu, *ACS Catal.*, 2018, **8**, 11330–11341.
42 D. Jung, M. H. Kim and J. Kim, *Org. Lett.*, 2016, **18**, 6300–6303.
43 Q. Yin and M. Oestreich, *Angew. Chem., Int. Ed.*, 2017, **56**, 7716–7718.

44 X. Ji, W.-Q. Liu, S. Yuan, Y. Yin, W. Ding and Q. Zhang, *Chem. Commun.*, 2016, **52**, 10555–10558.
45 S. W. M. Crossley, C. Obradors, R. M. Martinez and R. A. Shenvi, *Chem. Rev.*, 2016, **116**, 8912–9000.
46 J. R. Khusnutdinova and D. Milstein, *Angew. Chem., Int. Ed.*, 2015, **54**, 12236–12273.
47 A. M. Royer, T. B. Rauchfuss and D. L. Gray, *Organometallics*, 2010, **29**, 6763–6768.
48 A. Bartoszewicz, G. González Miera, R. O. Marcos, P.-O. Norrby and B. Martín-Matute, *ACS Catal.*, 2015, **5**, 3704–3716.
49 R. Wang, J. Ma and F. Li, *J. Org. Chem.*, 2015, **80**, 10769–10776.
50 C. Hou, Z. Zhang, C. Zhao and Z. Ke, *Inorg. Chem.*, 2016, **55**, 6539–6551.
51 S. Qu, Y. Dang, C. Song, M. Wen, K.-W. Huang and Z.-X. Wang, *J. Am. Chem. Soc.*, 2014, **136**, 4974–4991.
52 M. D. Wodrich and X. Hu, *Nat. Rev. Chem.*, 2017, **2**, 0099.
53 P. A. Dub, A. Matsunami, S. Kuwata and Y. Kayaki, *J. Am. Chem. Soc.*, 2019, **141**, 2661–2677.
54 S. M. Bellows, S. Chakraborty, J. B. Gary, W. D. Jones and T. R. Cundari, *Inorg. Chem.*, 2017, **56**, 5519–5524.
55 J. Nagy, Z. Madarász, R. Rapp, Á. Szöllösy, J. Nyitrai and D. Döpp, *J. Prakt. Chem.*, 2000, **342**, 281–290.

